Journal of Applied Polymer Science

Significantly Improving Electro-Activated Shape Recovery Performance of Shape Memory Nanocomposite by Self-Assembled Carbon Nanofiber and Hexagonal Boron Nitride

Haibao Lu, Ming Lei, Jinsong Leng
National Key Laboratory of Science and Technology on Advanced Composites in Special Environments, Harbin Institute of Technology, Harbin 150080, China
Correspondence to: H. Lu (E-mail: luhb@hit.edu.cn)

ABSTRACT: This study presents two effective approaches to significantly improve the electro-thermal properties and electro-activated shape recovery performance of shape memory polymer (SMP) nanocomposites that are incorporated with carbon nanofibers (CNFs) and hexagonal boron nitrides (h-BNs), and show Joule heating triggered shape recovery. CNFs were self-assembled and deposited into buckypaper form to significantly improve the electrical properties of SMP and achieve the shape memory effect induced by electricity. The h-BNs were either blended into or self-assembled onto CNF buckypaper to significantly improve the thermally conductive properties and electro-thermal performance of SMPs. Furthermore, the shape recovery behavior and temperature profile during the electrical actuation of the SMP nanocomposites were monitored and characterized. It was found that a unique synergistic effect of CNFs and h-BNs was presented to facilitate the heat transfer and accelerate the electro-activated shape recovery behavior of the SMP nanocomposites. © 2014 Wiley Periodicals, Inc. J. Appl. Polym. Sci. **2014**, *131*, 40506.

KEYWORDS: graphene and fullerenes; nanotubes; property relations; stimuli-sensitive polymers; structure

Received 18 December 2013; accepted 23 January 2014
DOI: 10.1002/app.40506

INTRODUCTION

Shape memory polymers (SMPs) belong to a class of polymeric smart materials that exhibit a drastic and discontinuous change in their shape or other physical properties with environmental conditions.[1–5] SMPs are characterized by the shape memory effect (SME), which is defined as the ability of a material to regain its original shape in the presence of the right stimulus.[1–6] However, the actual shape memory performance in a particular SMP is critically determined by its chemical structure, molecular weight, degree of cross-linking, fraction of amorphous and crystalline domains, etc.[7–10] SMPs can therefore retain two or sometimes three shapes, and the transition between those is sometimes induced by temperature.[7,8] There are numerous advantages that make SMPs more attractive in smart materials, such as high capacity for elastic deformation (up to 200% in most cases), low density, a broad range of tailorable transition temperature, easy processing and manufacturing techniques, potential biocompatibility, and biodegradability.[11–14] SMPs not only open an exciting field for many potential applications including medicine, aerospace, aircraft, textile, automobile, etc., but also bring forward a significant breakthrough in the development of advanced stimulus-responsive materials to complement or supplant traditional materials in a variety of applications.[15–17]

The research and development on the actuation approach for SMPs is one of the critical profiles to bridge the scientific development and practical engineering application. Thermally responsive SMP composites loaded with functional fillers can be triggered by means of indirect heating by electric current (Joule heating),[18–27] or magnetic field (inductive heating).[28,29] To achieve Joule heating, a small amount of conductive fillers, such as carbon nanotube,[18–20] carbon nanofiber (CNF),[21,22] carbon black,[23] electromagnetic particle,[24,25] electrically conductive hybrid fiber,[26] and continuous conductive carbon fiber[27] have been applied. However, how to effectively integrate nanosized particles into SMPs for high performance is still an open question at this moment. The resulting electrical conductivity of SMP composites is still relatively low, primarily due to the lack of effective techniques to achieve a perfect dispersion and form continuously conductive networks by the conductive fillers. Various strategies, including surface modification or treatment, *in situ* polymerization, applying high aspect ratio particles, or aligning particles by electromagnetic field, have been introduced and employed.[19,20,23,25,26,29] Recently, continuous carbon fiber, CNF mat, carbon-based

buckypaper, and functionalized graphene sheet have been explored for the actuation of SMPs via electrically resistive Joule heating.[30–34] However, the interface issue between the conductive part and the SMP matrix occurs during shape recovery resulting from the large dissimilarity in their thermal properties. Consequently, the efficiency of heat transfer from the conductive part to the SMP part is limited. Furthermore, the life and repeatability of the SMP composites could not be guaranteed. On these motivations, this study presents two effective approaches to significantly improve the electro-thermal properties and electro-activated shape recovery performance of SMP nanocomposites that are incorporated with CNFs and hexagonal boron nitrides (h-BNs) and show Joule heating triggered shape recovery. CNFs were self-assembled and deposited into buckypaper form to significantly improve the electrical properties of SMP and achieve the SME induced by electricity. The h-BNs were either blended into or self-assembled onto CNF buckypaper to significantly improve the thermally conductive properties and electro-thermal performance of SMPs. Furthermore, the shape recovery behavior and temperature profile during the electrical actuation of the SMP nanocomposites were monitored and characterized. It was found that a unique synergistic effect of CNFs and h-BNs was presented to facilitate the heat transfer and accelerate the electro-activated shape recovery behavior of the SMP nanocomposites.

EXPERIMENTAL

The SMP matrix used in this study was a thermosetting epoxy-based shape memory resin with a density of 1.00 g cm^{-3} and a curing temperature of 150°C. The epoxy-based SMP was synthesized by using the aromatic diepoxide, aliphatic diepoxy, and diamine. In the epoxy-based SMP, the aromatic diepoxide works as rigid segment and plays the role in memorizing the permanent shape, the aliphatic diepoxy works as soft segment and plays the role in changing shape in response to the external stimulus, and the diamine is the curing agent. The epoxy resin and the diamine have a molecular weight ratio of 2 : 5 in synthesis. The cured epoxy-based SMP has unique "shape memory" properties. And the shape fixity is of 100%, shape recovery ratio is of >99%, and the shape transition temperature is of 102°C. It combines shape memory properties with high toughness and good strength of epoxy. CNFs were received in powder form and heat treated at 2200°C to obtain complete graphitic structures and purify themselves to a very high level (>99 wt %). The nanofibers have a diameter of 50–100 nm and a length of 30–100 μm. The electrical conductivity of the CNFs is 0.75 S cm^{-1}. Boron nitride particles are obtained by reacting boron trioxide (B_2O_3) with urea ($CO(NH_2)_2$) in a nitrogen atmosphere at a temperature of 1600°C to achieve a high concentration of >98%. h-BN is isoelectronic to a similarly structured carbon lattice. Thermal conductivity and thermal expansion coefficients of h-BN are 600 W/m K and -2.7×10^{-6}/°C, respectively.

In the fabrication of buckypaper, the CNFs or h-BNs were divided into several parts evenly, and then transferred into 1000 mL beakers. Then 600 mL of water was added in each beaker, along with 4 mL of nonionic surfactant $C_{14}H_{22}O(C_2H_4O)_n$ (Triton X-100). The solution was subsequently sonicated using a high-intensive probe sonicator for 15 min. After which, the solution was cooled down to room temperature and sonicated once again for another 15 min. Consequently, the as-prepared suspensions were transferred into a filtration system. Self-assembly is a type of process in which a disordered system of pre-existing components forms an organized structure or pattern as a consequence of specific, local interactions among the components themselves, without external direction. Therefore, CNF or h-BN particles were self-assembled into the buckypaper that was made by filtering the suspension through a 0.4 μm hydrophilic polycarbonate membrane under a high pressure (0.689 MPa) in the filtration system. The buckypaper was put into a heating oven at a temperature of 120°C for 2 h to further remove the remaining water and surfactant. The resin transfer molding technique was used to make the SMP nanocomposite. Two types of buckypaper enabled SMP nanocomposite were prepared. The first one consisted of the h-BNs being self-assembled onto CNF buckypaper and then incorporated into the SMP matrix. The second one involves the h-BNs being blended into the CNF buckypaper and then incorporated into the SMP matrix. The curing cycle for the resin transpired as follows: the resin mixture was first ramped up to 100°C at a heating rate of 1°C/min and held for 5 h, and then it was ramped up to 120°C at a heating rate of 1°C/min and held for another 3 h, finally it was ramped up from 120°C to 150°C at a heating rate of 30°C per 120 min to produce the final SMP nanocomposite.

RESULTS AND DISCUSSION

Morphology and Structure of CNF and h-BN in Buckypaper

The morphology and structure of the CNF and h-BN in buckypaper were characterized by using field emission scanning electron microscopy (FESEM) at an accelerating voltage of 20.00 keV. The morphology and structure of the CNF are presented in Figure 1(a). The CNFs were homogeneously dispersed without any aggregation. CNFs are one of the best conductive materials, each individual CNF provides a conductive path for electrons. The continuous network structure could transform a nonconductive polymer to be a conductor through the conductive network and therefore enhance the conductivity. The morphology and structure of the h-BNs are presented in Figure 1(b). They exhibit a plate-like microstructure and layered lattice structure that is similar to the structure of carbon graphene.[35] Meanwhile, it was found that a network structure was formed by molecular interaction and mechanical interlocking among individual h-BNs in the buckypaper. The h-BNs are expected to appropriately enhance the electrical resistivity to increase and facilitate the electrically resistive Joule heating of CNFs. Figure 1(c,d) present the morphology and structure of CNF and h-BN hybrid. The images from an optical microscope were captured by a charge-coupled device (CCD) camera for the CNF buckypaper and CNF/BN buckypaper enabled SMP nanocomposites, as shown in Figure 2(a,b). For the CNF buckypaper enabled nanocomposite

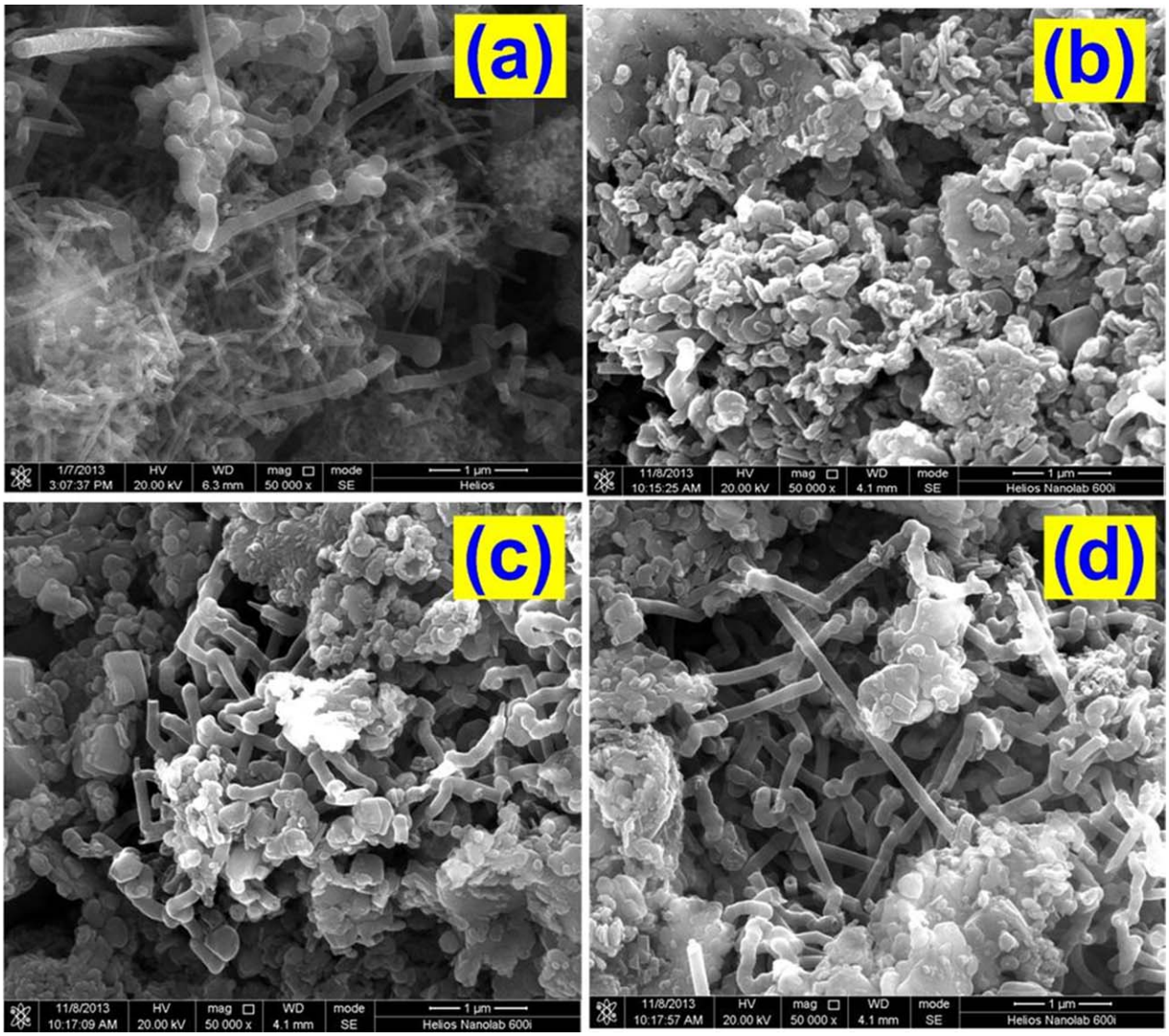

Figure 1. (a,b) Morphology and network structure of CNFs and h-BNs in buckypaper recorded by the SEM at a scale of 1 μm, respectively. (c,d) Morphology and structure of CNF and h-BN hybrid in buckypaper. [Color figure can be viewed in the online issue, which is available at wileyonlinelibrary.com.]

blended with h-BNs into buckypaper, the transparency of the matrix became poor, as shown in Figure 2(b).

Fourier Transform Infrared (FTIR) Spectroscopy

Figure 3 compares the Fourier transform infrared (FTIR) spectra (Nicolet AVATAR 360) of nanocomposites with 0.10 and 0.14 g CNFs as well as 0.08 g CNFs with 0.02 g h-BNs and 0.06 g h-BNs buckypaper, in the range from 4000 to 400 cm^{-1}. Ill-organized graphitic and aminated-CNF lead to the appearance of a series of bands with a maximum transmittance at 1389 cm^{-1} as D-band and 796 cm^{-1} as aminated-CNF, respectively. The D bonding of C=C ranged from 1378 to 1389 cm^{-1} with a change in the concentration of CNF and concentration ratio of CNF to h-BN due to the change in their mechanical attractive force.

Electrical Resistivity Measurement

The electrical resistivity of the buckypapers was obtained by using a van der Pauw four-point probe method that is based on an electrical impedance measuring technique and uses separate pairs of current-carrying and voltage-sensing electrodes. To make a measurement, an electric current is caused to flow along one edge of the specimen, while the voltage across the opposite edge is measured. From these two values, a resistance can be found using Ohm's law. The experimental results of each tested specimen were measured twenty times by the two modes (Mode I and Mode II as shown in the insert image in Figure 4). Figure 4 compares the resistivity of the CNF/BN buckypapers with weight concentration of 55.6%, 66.7%, 77.8%, 88.9%, and 100% of CNFs. While one series is only incorporated of CNFs, the others contain CNFs and h-BNs. As is shown, with the increase in CNF content in the buckypaper, electrical resistivity gradually decreases. The average electrical resistivity decreased from 0.05892 to 0.04316 ohm·cm for the CNF buckypaper. The effect of h-BN and CNF on the average electrical resistivity of buckypaper presents a unique synergistic effect. The average electrical resistivity decreased from 0.09543

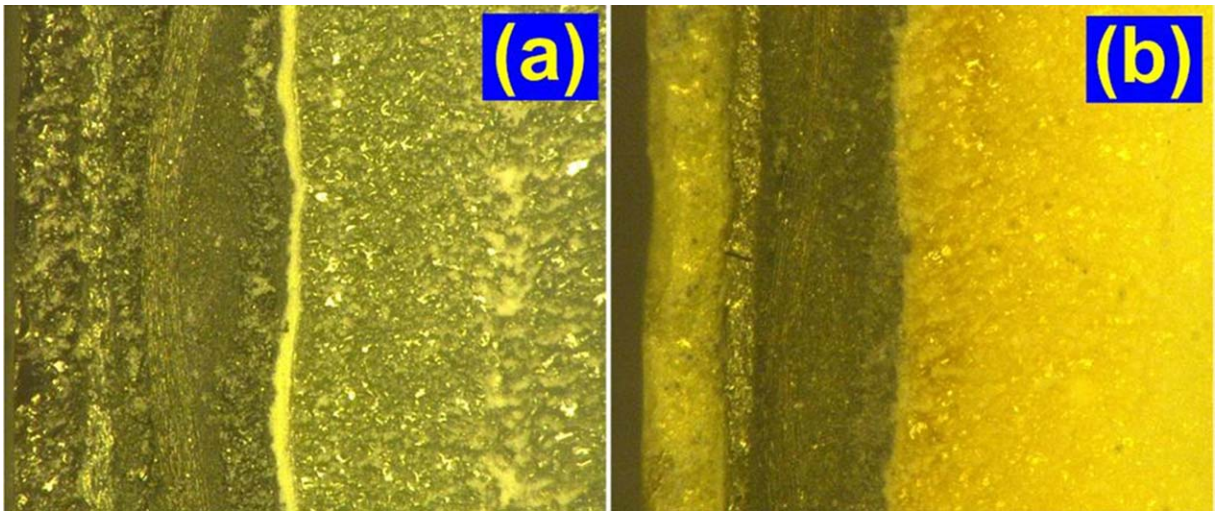

Figure 2. (a) Morphology of CNF/BN buckypaper enabled SMP nanocomposite by the optical microscope at a magnification of ×200 and (b) Morphology of CNF buckypaper-enabled SMP nanocomposite blended with h-BNs by the optical microscope at a magnification of 200×. [Color figure can be viewed in the online issue, which is available at wileyonlinelibrary.com.]

to 0.06911 ohm·cm, as the weight centent of h-BN increased from 11.1% to 44.4%. After that it increased from 0.06911 to 0.07636 ohm cm, as the weight of h-BN further increased from 44.4% to 55.6%. The experimental results present that the average electrical resistivity of CNF buckypaper is lower than that of CNF/BN buckypaper at the same weight concentration. When the buckypaper contains a relatively low weight concentration of CNFs, the volume fraction of the pores in the buckypaper is high. When the pores are filled by the insulating h-BNs with a proper content, the conductive network could not be destroyed or obstructed. Therefore, the electrical resistivity of the buckypapers could be lowered due to their high density. However, the conductive CNF network could be damaged with the more h-BN particles added in the buckypaper. Here, insulating h-BN particles permeated into and loosened the conductive CNF network. Hence, the distance of the electric current is increased. On the other hand, the cross-sectional area of the buckypaper increased as the h-BNs were deposited onto the CNFs. This increase in electrical resistivity was found with the Ohm's law.

Electrically Induced Shape Recovery Behavior

In order to demonstrate the shape recovery induced by Joule heating, two specimens (namely CNF/BN buckypaper enabled SMP nanocomposite, and CNF buckypaper enabled SMP nanocomposite (with the h-BNs blended into the CNF buckypaper)). The flat (permanent shape) nanocomposite specimen with a dimension of 60 × 4.5 × 1 mm^3 was bent into an "n"-like shape (temporary shape) at 160°C, and then cooled back to a room temperature of 22°C. No apparent shape recovery was found after the deformed specimen was kept in air for 60 min. Subsequently, 0.48 Å of electric current was applied on the tested specimens. Both video and infrared video cameras were used to record and monitor the shape recovery [as shown Figure 4(a,c)] and temperature distribution [as shown Figure 4(b,d)] simultaneously. Figure 5 illustrates the electrically induced shape recovery with four snap shots of each specimen. It is found that CNF/BN buckypaper enabled specimen completed the Joule heating-induced shape recovery in the short time of 80 s. While that of the CNF buckypaper enabled specimen was 132 s. Finally, the nanocomposite specimen did not show a 100% recovery ratio. This recovery ratio loss could be resulted from the interfacial friction between buckypaper and the underlying SMP matrix. The SMP part couldn't provide enough mechanical loading to pull the buckypaper to return to the original flat shape. Additionally, the relative motion of macromolecule segments is the primary mechanism of the SME in SMP. The size of h-BNs is of the same order as the typical segments of the SMP. Therefore, the frictional interaction between the macromolecule segments and h-BNs

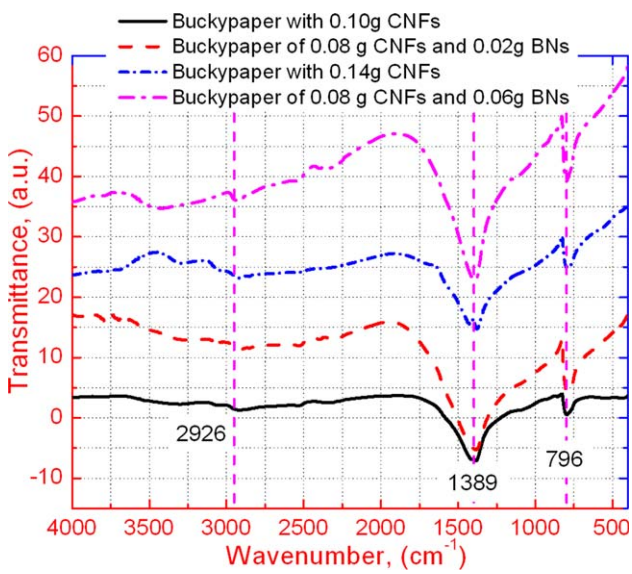

Figure 3. FTIR spectra of the CNF buckypaper attached nanocomposites measured in a transmittance mode. [Color figure can be viewed in the online issue, which is available at wileyonlinelibrary.com.]

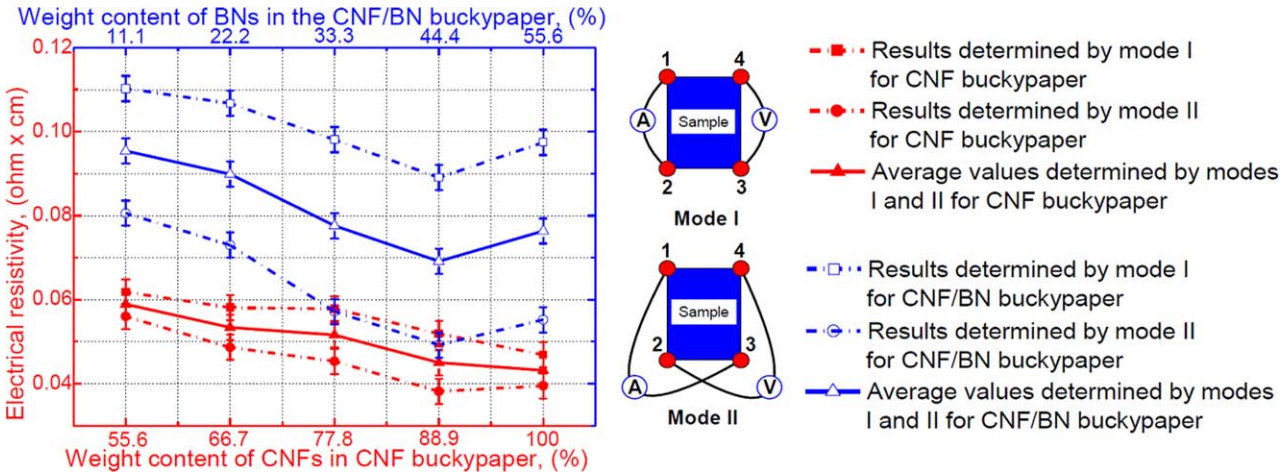

Figure 4. Electrical resistivity of CNF and CNF/BN buckypapers as a function of weight concentration. Insets: measurement Mode I and Mode II. [Color figure can be viewed in the online issue, which is available at wileyonlinelibrary.com.]

could also reduce the shape recovery ratio of the SMP nanocomposite.

Temperature distribution along a specific line (left-top inset) on the specimen (at 10 selected points) was plotted in Figure 6. High temperatures were found where internal strains were higher than the local resistivity. With electricity being applied, the resistive Joule heating resulted in the temperature gradually increased. We can see that the CNF/BN buckypaper enabled nanocomposite specimen reached the higher temperature of 184.76°C at multiple locations, while the temperature of the CNF buckypaper enabled specimen was at 87.28°C. Experimental results present that the temperature of the tested SMP nanocomposite incorporated with CNF/BN buckypaper is higher than that of the nanocomposite with CNF buckypaper, where the SMEs of them both were induced by a constant electric current of 0.48 Å. At the same heating time of 30, 60, and 80 s, more resistive Joule heating results in the high temperature and temperature profile against all the selection location in the CNF/BN buckypaper enabled nanocomposite specimen. Because of the synergistic effect of

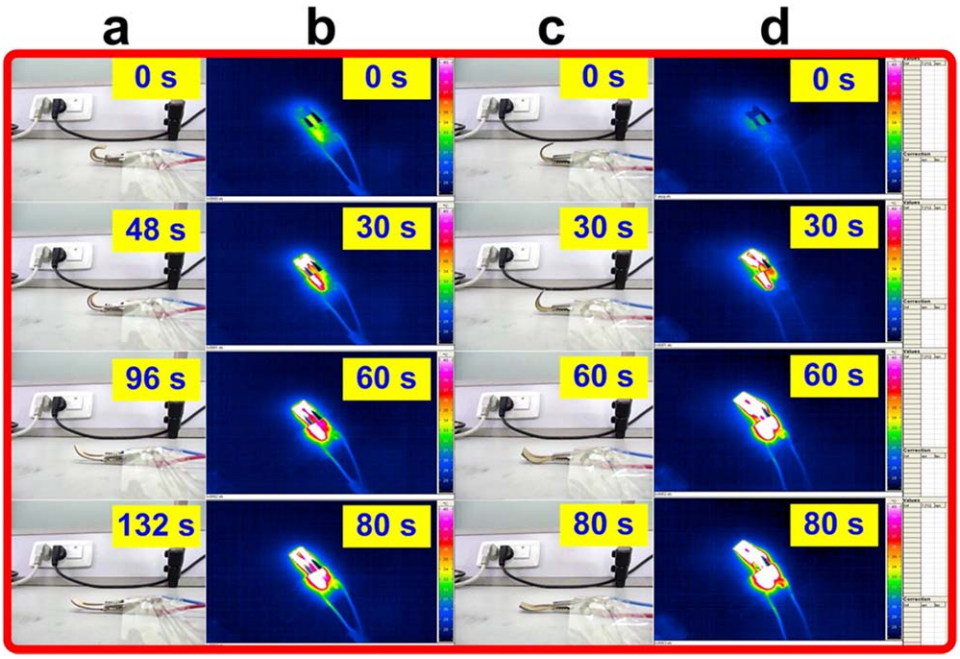

Figure 5. Snapshot of the Joule heating-induced SME in SMP nanocomposite. (a) Shape recovery was recorded by the video camera for the specimen enabled with CNF buckypaper and blended with h-BNs. (b) Shape recovery and temperature distribution were simultaneously record by the infrared video camera for the specimen enabled with CNF buckypaper and blended with h-BNs. (c) Shape recovery was recorded by the video camera for the specimen enabled with CNF/BN buckypaper. (d) Shape recovery and temperature distribution were simultaneously record by the infrared video camera for the specimen enabled with CNF/BN buckypaper. [Color figure can be viewed in the online issue, which is available at wileyonlinelibrary.com.]

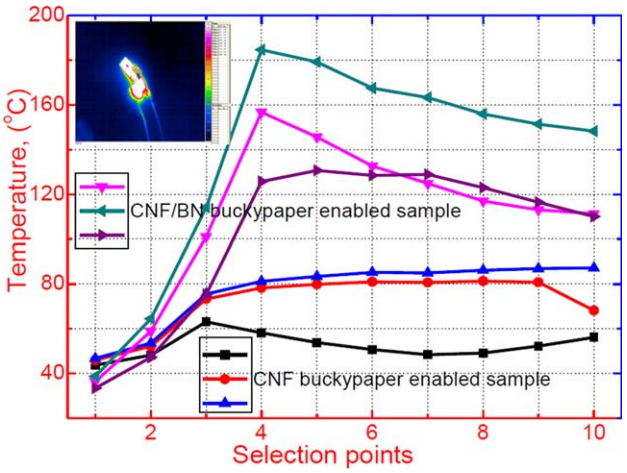

Figure 6. Temperature distribution curves of the SMP nanocomposites driven by Joule heating at a heating time of 30, 60, and 80 s, respectively. The curves marked by black, red, and blue color are for the CNF buckypaper enabled SMP nanocomposite specimen at a heating time of 30, 60, and 80 s, respectively. The curves marked by pink, green, and violet color are for the CNF/BN buckypaper enabled SMP nanocomposite specimen at a heating time of 30, 60, and 80 s, respectively. Inset: the infrared image to present the 10 selection locations on the tested specimen. [Color figure can be viewed in the online issue, which is available at wileyonlinelibrary.com.]

CNF and h-BN on the electrical resistivity of buckypaper, the heating efficiency was significantly improved in comparison to that of the CNF buckypaper enabled SMP nanocomposite. The CNFs help to significantly improve the electrical conductivity, and the h-BNs significantly improve the thermally conductive properties of the SMP matrix. Therefore, the synergistic effect of the electrical and thermal conductive property of the buckypaper plays a critical and essential role in influencing the Joule heating-induced shape recovery of SMPs.

CONCLUSIONS

This article presented two effective approaches to significantly improve the electro-thermal properties and electro-activated shape recovery performance of epoxy-based SMP nanocomposites incorporated with CNFs and h-BNs. CNFs were self-assembled and deposited into buckypaper form to lower the electrical resistivity of an SMP to 0.04316 ohm cm. The h-BNs were either blended or self-assembled into buckypaper on the CNFs to improve the thermal conductivity. A unique synergistic effect of CNFs and h-BNs was presented to facilitate the heat transfer and accelerate the electro-activated shape recovery behavior of the SMP nanocomposites in 80 s, with an electric current of 0.48 A. We demonstrated that a simple way to produce electro-activated SMP nanocomposites by application of buckypaper through electrically resistive Joule heating.

ACKNOWLEDGMENTS

This work was supported by the National Natural Science Foundation of China (NSFC) (Grant No. 51103032), Fundamental Research Funds for the Central Universities (Grant No. HIT.BRETIV.201304) and China Postdoctoral Science Foundation (Grant No. 20110490104 and 2012T50350).

REFERENCES

1. Lendlein, A.; Jiang, H.; Jünger, O.; Langer, R. *Nature (London)* **2005**, *434*, 879.
2. Xie, T. *Nature(London)* **2010**, *464*, 267.
3. Wang, C. C.; Huang, W. M.; Ding, Z.; Zhao, Y.; Purnawali, H. *Compos. Sci. Technol.* **2012**, *72*, 1178.
4. Mather, P. T.; Luo, X. F.; Rousseau, I. A. *Annu. Rev. Mater. Res.* **2009**, *39*, 445.
5. Meng, Q.; Hu, J. *Compos. Part A-Appl. S.* **2009**, *40*, 1661.
6. Huang, W. M.; Ding, Z.; Wang, C. C.; Wei, J.; Zhao, Y.; Purnawli, H. *Mater. Today* **2010**, *13*, 54.
7. Kim, B. K.; Lee, S. Y.; Xu, M. *Polymer* **1996**, *37*, 5781.
8. Bellin, I.; Kelch, S.; Langer, R.; Lendlein, A. P. *Natl. Acad. Sci. USA* **2006**, *103*, 18043.
9. Buckley, C. P.; Prisacariu, C.; Caraculacu, A. *Polymer* **2007**, *48*, 1388.
10. Park, C.; Lee, J. Y. *J. Appl. Polym. Sci.* **2004**, *94*, 308.
11. Hu, J. L.; Zhu, Y.; Huang, H. H.; Lu, J. *Prog. Polym. Sci.* **2012**, *37*, 1720.
12. Meng, H.; Li, G. Q. *Polymer* **2013**, *54*, 2199.
13. Zhao, Q.; Behl, M.; Lendlein, A. *Soft Matter* **2013**, *9*, 1744.
14. Lu, H. B.; Huang, W. M.; Yao, Y. T. *Pigm. Resin Technol.* **2013**, *42*, 237.
15. Lendlein, A.; Langer, R. *Science* **2002**, *296*, 1673.
16. Yakacki, C. M.; Shandas, R.; Lanning, C.; Rech, B.; Eckstein, A.; Gall, K. *Biomaterials* **2010**, *28*, 2255.
17. Lantada, A. D.; Morgado, P. L.; Sanz, J. L. M.; García, J. M.; Munoz-Guijosa, J. M.; Otero, J. E. *Smart Mater. Struct.* **2010**, *19*, 055022.
18. Cho, J. W.; Kim, J. W.; Jung, Y. C.; Goo, N. S. *Macromol. Rapid Commun.* **2005**, *26*, 412.
19. Lu, H. B.; Bai, P. P.; Yin, W. L.; Liang, F.; Gou, J. H. *Nanosci. Nanotech. Lett.* **2013**, *5*, 732.
20. Xiao, Y.; Zhou, S. B.; Wang, L.; Gong, T. *ACS Appl. Mater. Interfaces* **2010**, *2*, 3506.
21. Koerner, H.; Price, G.; Pearce, N. A.; Alexander, M.; Vaia, R. A. *Nat. Mater.* **2004**, *3*, 115.
22. Tang, Z.; Sun, D.; Yang, D.; Guo, B.; Zhang, L.; Jia, D. *Compos. Sci. Technol.* **2013**, *75*, 15.
23. Le, H. H.; Zulfiqar, A.; Mathias, U.; Ilisch, S.; Radusch, H. J. *J. Appl. Polym. Sci.* **2011**, *120*, 2138.
24. Lu, H. B.; Gou, J. H.; Leng, J. S.; Du, S. Y. *Appl. Phys. Lett.* **2011**, *98*, 174105.
25. Lu, H. B.; Gou, J. H.; Leng, J. S.; Du, S. Y. *Smart Mater. Struct.* **2011**, *20*, 035017.
26. Leng, J. S.; Lv, H. B.; Liu, Y. J.; Du, S. Y. *J. Appl. Phys.* **2008**, *104*, 104917.

27. Lu, H. B.; Yin, W. L.; Huang, W. M.; Leng, J. S. *RSC Adv.* **2013**, *3*, 21484.
28. Schmidt, A. M. *Macromol. Rapid Commun.* **2006**, *27*, 1168.
29. Buckley, P. R.; McKinley, G. H.; Wilson, T. S.; Small, W.; Benett, W. J.; Bearinger, J. P.; McElfresh, M. W.; Maitland, D. *J. IEEE Trans. Biomed. Eng.* **2006**, *53*, 2075.
30. Luo, X. F.; Mather, P. T. *Soft Matter* **2010**, *6*, 2146.
31. Lu, H. B.; Liu, Y. J.; Leng, J. S.; Du, S. Y. *Smart Mater. Struct.* **2010**, *19*, 075021.
32. Lu, H. B.; Liu, Y. J.; Leng, J. S.; Du, S. Y. *Appl. Phys. Lett.* **2010**, *96*, 084102.
33. Lu, H. B.; Liang, F.; Gou, J. H. *Soft Matter* **2011**, *7*, 7416.
34. Lu, H. B.; Huang, W. M. *Appl. Phys. Lett.* **2013**, *102*, 231910.
35. Lu, H. B.; Gou, J. H. *Nanosci. Nanotech. Lett.* **2012**, *4*, 1155.